# GENERALIZED MOMENTUM DISTRIBUTION OF NUCLEAR MATTER

J.W. CLARK

McDonnell Center for the Space Sciences
and Department of Physics
Washington University
St. Louis, MO 63130, USA

E. MAVROMMATIS AND M. PETRAKI

Physics Department, Division of Nuclear and Particle Physics
University of Athens
Panepistimioupoli, 15771 Athens, Greece

*(Received February 9, 1993)*

*Dedicated to Janusz Dąbrowski in honour of his 65th birthday*

The half-diagonal two-body density matrix $\rho_2(r_1, r_2, r_1', r_2')$ is studied in infinite nuclear matter, based on Jastrow–Slater ground-state trial functions. The associated generalized momentum distribution $n(\boldsymbol{p}, \boldsymbol{Q})$, related to the half-diagonal version of $\rho_2$ by Fourier transformation in the variables $r_1 - r_1'$ and $r_1 - r_2$, is calculated for three representative models of nuclear matter containing central correlations. The available numerical results correspond to (a) approximation in lowest (two-body) cluster order of a straightforward cluster expansion of the generalized momentum distribution and (b) evaluation, to lowest cluster order, of form factors and other ingredients of a re-summed structural expression for $n(\boldsymbol{p}, \boldsymbol{Q})$ that collects the effects of different virtual scattering processes in the many-body medium. Dynamical correlations produce significant departures from the reference case of an ideal Fermi gas. The results should give an adequate picture of the behavior of $n(\boldsymbol{p}, \boldsymbol{Q})$ in certain limiting domains of the momenta $\boldsymbol{p}$ and $\boldsymbol{Q}$ where the short-range correlations dominate the complicated effects arising from the state-dependence of the interaction.

PACS numbers: 21.65. +f, 24.10. Cn, 67.50. -b, 67.50. Dg

## 1. Introduction

Among his many pioneering contributions to nuclear many-body theory and hadronic physics, Janusz Dąbrowski can count the first studies of a finite nucleus with a Jastrow-correlated trial ground state [1, 2]. In the thirty-odd years since papers [1, 2] were written in Peierls' department at Birmingham, there have been enormous developments in *ab initio* calculation of nuclear properties, within the conventional picture of a system of nonrelativistic nucleons interacting via two- (and three-) body interactions fitted to few-nucleon data. These developments were stimulated by striking advances in experiment and observation, ranging from high-energy electron scattering to measurements of post-glitch relaxation in neutron stars. A powerful arsenal of many-body procedures has become available, including Brueckner–Bethe–Goldstone theory [3] (to which Janusz also made seminal contributions), the self-consistent Green's function approach [4], the coupled-cluster method [5], stochastic or Monte Carlo computational algorithms [6] and, of course, correlated-basis or CBF theory [7–10]. The current generation of *ab initio* calculations on nuclei and nuclear matter are yielding a convincing quantitative picture of the correlation structure and dynamical response of nuclei, as exemplified by recent progress on single-nucleon spectral functions [11–14]. Even so, the essential features of Dąbrowski's original variational calculation of the $^{16}$O ground state are quite recognizable in its modern reincarnation: the large-scale computational effort of the Argonne–Urbana group [15] involving state-dependent correlations and Monte Carlo evaluation of cluster diagrams.

Let $\Psi(r_1, r_2, r_3 ... r_A)$ denote the unit-normalized ground-state wave function of a strongly interacting quantum system such as liquid $^4$He or liquid $^3$He, nuclear or neutron matter, or a finite nucleus. The associated two-body density matrix, defined by

$$\rho_2(r_1, r_2, r_1', r_2') = A(A-1) \int \Psi^*(r_1, r_2, r_3 \dots r_A) \Psi(r_1', r_2', r_3 \dots r_A) dr_3 \cdots dr_A, \qquad (1)$$

contains a wealth of information on the correlation structure of the many-body medium. (Spin/isospin labels are left implcit, as is a sum over all spin/isospin variables.) This function supplies the microscopic input for a number of fundamental sum rules (investigated systematically by Stringari [16]) that illuminate the "density fluctuation" and "single-particle" nature of the elementary excitations in Bose superfluids. In particular, the half-diagonal version $\rho_{2h}(r_1, r_2, r_1')$ of the two-body density matrix (1), with $r_2' = r_2$, puts constraints on the importance of multiparticle-multihole excitations through the $\omega^2$ sum rule [7, 17]. The quantity $\rho_{2h}$ is also expected to

play a prominent role in the corresponding sum rules for Fermi systems including nuclear matter. Furthermore, $\rho_{2h}$ is an essential structural input for theories of final-state effects in deep-inelastic neutron scattering from liquid $^4$He and in quasielastic electron-nucleus scattering [18, 19]. Such theories provide a basis for quantitative prediction of the dynamic structure function at high momentum transfer, and for determination of the ground-state momentum distribution from experimental scattering data.

Indeed, there is rising interest in the two-body density matrix of finite nuclei. This interest is spurred by the fact that proper interpretation of a range of recent or planned experiments, in new or projected facilities, is contingent on the availability of a more quantitative, "post-mean-field" treatment of the propagation of ejected nucleons and their final-state interactions (FSI). Attention is focused on inclusive quasielastic $(e, e')$ scattering [20] as well as exclusive quasielastic $(e, e'N)$ [21] and $(e, e'2N)$ events. In these electronuclear processes, FSI can have a significant influence at low energy transfer even for beam energies in the multi-GeV region. Reliable extraction of the momentum distributions, spectral functions and transparency from the experimental data therefore requires an accurate accounting of final-state effects. In addition to electron scattering, FSI are involved in proton scattering $(p, 2p)$ [22] and pion absorption [23] experiments. As we progress beyond mean-field, optical-model approximations, theoretical treatments of FSI are found to involve the diagonal and half-diagonal portions of the two-body density matrix. Notable examples include the extensions of Glauber theory [24, 25], adaptation of Silver's hard-core perturbation theory to the nuclear medium [26] and other approaches under current discussion [27, 28].

Ristig and Clark have carried out rather general asymptotic and diagrammatic analyses of the half-diagonal density matrices of strongly interacting Bose and Fermi systems (and of the full Bose $\rho_2$) and developed methods for their quantitative microscopic evaluation [29, 30]. Both cluster-expansion [31] and hypernetted-chain (HNC) [8] techniques are available when the wave function is of the conventional Jastrow form. The formal structural analysis of the half-diagonal two-body density matrix is pursued most efficiently in the configuration-space representation. A diagrammatic cluster expansion of $\rho_{2h}$ is generated and then graphical resummations performed using hypernetted-chain algorithms. On the other hand, the physical meaning of the results is more vividly described in the momentum representation, *i.e.*, in terms of the so-called *generalized momentum distribution*

$$n(\boldsymbol{p}, \boldsymbol{Q}) = \sum_{\hat{k}} \langle \Psi | a^\dagger_{\hat{k}+\boldsymbol{Q}} a^\dagger_{\hat{p}-\boldsymbol{Q}} a_{\hat{p}} a_{\hat{k}} | \Psi \rangle \,, \tag{2}$$

which is related to the configuration-space density matrix $\rho_{2h}(\boldsymbol{r}_1, \boldsymbol{r}_2, \boldsymbol{r}'_1)$ by Fourier transformation. (Here, $\hat{k}$ denotes the single-particle orbital with

quantum numbers $\boldsymbol{k}, \sigma$, where $\boldsymbol{k}$ is the wave vector or momentum and $\sigma$ is the spin projection, while $\hat{\boldsymbol{k}} + \boldsymbol{Q} = (\boldsymbol{k} + \boldsymbol{Q}, \sigma)$.) In detail, the relevant Fourier transformation is

$$n(\boldsymbol{p}, \boldsymbol{Q}) = \frac{1}{\nu} \frac{\rho}{A} \int \rho_{2h}(\boldsymbol{r}_1, \boldsymbol{r}_2, \boldsymbol{r}_1') \mathrm{e}^{-i\boldsymbol{p}\cdot(\boldsymbol{r}_1 - \boldsymbol{r}_1')} \mathrm{e}^{-i\boldsymbol{Q}\cdot(\boldsymbol{r}_1 - \boldsymbol{r}_2)} d\boldsymbol{r}_1 d\boldsymbol{r}_2 d\boldsymbol{r}_1' \,, \quad (3)$$

where $A$ is the number of nucleons, $\nu$ is the single-particle level degeneracy (4 for nuclear matter) and $\rho$ is the (uniform) density of the system, connected to the Fermi wave number $k_{\mathrm{F}}$ through $\rho = \nu k_{\mathrm{F}}^3 / 6\pi^2$. In the absence of dynamical and statistical correlations, the generalized momentum distribution function collapses to the elementary result

$$n_o^o(\boldsymbol{p}, \boldsymbol{Q}) = \delta_{Q0}(A-1) n^o(p) \,, \quad (4)$$

where $n^o(p)$ is the single-particle momentum distribution assumed for the noninteracting system of distinguishable particles. Considering a noninteracting system of fermions with level degeneracy $\nu$, the Pauli exclusion principle generates kinematic correlations between particles of the same spin projection, and $n(\boldsymbol{p}, \boldsymbol{Q})$ becomes

$$n_F(\boldsymbol{p}, \boldsymbol{Q}) = \delta_{Q0}(A-1)\Theta(k_{\mathrm{F}} - p) - (1 - \delta_{Q0})\Theta(k_{\mathrm{F}} - p)\Theta(k_{\mathrm{F}} - |\boldsymbol{p} - \boldsymbol{Q}|) \,. \quad (5)$$

Clearly, for $Q = 0$ any deviation of $n(\boldsymbol{p}, \boldsymbol{Q})$ from zero when $p$ is outside the Fermi sea is indicative of the presence of dynamical correlations; likewise dynamical correlations are indicated for $Q \neq 0$ when $n(\boldsymbol{p}, \boldsymbol{Q})$ is nonzero at $\boldsymbol{p}$ values satisfying $p > k_{\mathrm{F}}$ or $|\boldsymbol{p} - \boldsymbol{Q}| > k_{\mathrm{F}}$.

The role of $n(\boldsymbol{p}, \boldsymbol{Q})$ in quasielastic electron scattering from a system of nucleons becomes more concrete when we write this quantity as

$$n(\boldsymbol{p}, \boldsymbol{Q}) = \langle \Psi | \rho_{\boldsymbol{Q}} a^\dagger_{\hat{\boldsymbol{p}} - \boldsymbol{Q}} a_{\hat{\boldsymbol{p}}} | \Psi \rangle - n(p) \,, \quad (6)$$

where $\rho_{\boldsymbol{Q}}$ is the density fluctuation operator $\sum_{\hat{k}} a^\dagger_{\hat{k}+\boldsymbol{Q}} a_{\hat{k}}$ (with $Q \neq 0$) and $n(p)$ is the single-particle momentum distribution function. The first term on the right in Eq. (6) may be interpreted as a transition matrix element for scattering of a particle out of orbital $\hat{\boldsymbol{p}} = (\boldsymbol{p}, \sigma')$ into another orbital $\hat{\boldsymbol{p}} - \boldsymbol{Q} = (\boldsymbol{p} - \boldsymbol{Q}, \sigma')$, the process being mediated by a density fluctuation of wave vector $\boldsymbol{Q}$. Thus, an evaluation of $n(\boldsymbol{p}, \boldsymbol{Q})$ amounts to a calculation of the rightmost single-nucleon vertex in the Fig. 1. (It should be pointed out, however, that in nuclear problems other final-state interaction mechanisms may be more important than the phonon-induced process of Fig. 1, depending on the momentum and energy transfers involved.)

We may further observe that simple operations determine the radial distribution function $g(r_{12})$ and the one-body density matrix $\rho_1(\boldsymbol{r}_1, \boldsymbol{r}_1')$ or

single-particle momentum distribution $n(p)$ from the half-diagonal two-body density matrix or its corresponding generalized momentum distribution. In the full diagonal case ($r_1' = r_1$ as well as $r_2' = r_2$), Eq. (1) reproduces the definition of the radial distribution function, so that

$$\rho_{2h}(r_1, r_2, r_1) = \rho^2 g(r_{12}) . \tag{7}$$

Alternatively, summing Eq. (3) over $\hat{p}$ we arrive at the so-called $p$ sum rule [29],

$$\begin{aligned} A^{-1} \sum_{\hat{p}} n(p, Q) &= A\delta_{Q0} + \rho \int [g(r_{12}) - 1] e^{-iQ \cdot r_{12}} dr_{12} \\ &= A\delta_{Q0} + [S(Q) - 1] , \end{aligned} \tag{8}$$

where $S(Q)$ is the static structure function (and of course $r_{12} = r_1 - r_2$). We may assume that the short-range repulsions are strong enough that $g(r_{12})$ vanishes at zero distance. Summing Eq. (2) over $Q$ we then obtain the $Q$ sum rule [29],

$$\sum_{Q} n(p, Q) = 0 . \tag{9}$$

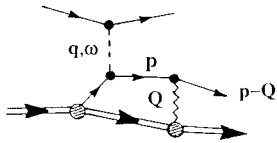


Fig. 1. Deep-inelastic scattering of a probe from a normal quantum fluid, involving final-state interaction between an ejected particle of the fluid and the residual system, mediated by a density fluctuation (phonon) of momentum $Q$.

The sequential relation [7]

$$\int \rho_{2h}(r_1, r_2, r_1') dr_2 = (A - 1)\rho_1(r_1, r_1') \tag{10}$$

serves to connect $n(p, Q)$ with the single-particle momentum distribution $n(p)$. In momentum space this relation is just

$$n(p, Q = 0) = (A - 1)n(p) . \tag{11}$$

There exists a substantial body of work directed to microscopic evaluation of the momentum distribution $n(p)$ and one-body density matrix $\rho_1(r_1, r_1')$ in nuclear matter (see *e.g.* [32–36, 12]) and finite nuclei (*e.g.* [37,

38]). Quantitative information on the two-body density matrix and associated generalized momentum distribution is rather more limited. Prior to the work of Ristig and Clark [29, 30], three simple prescriptions [39] were proposed (by Gersch and coworkers, by Silver, and by Rinat) for estimating the half-diagonal density matrix, with special focus on the problem of final-state interactions in neutron scattering from the helium liquids. In [29, 30] cluster expansions of $n(\boldsymbol{p}, \boldsymbol{Q})$ were formally re-summed for both Bose and Fermi trial ground states of Jastrow type, in terms of a set of form factors, and the two-point form factors were calculated in liquid $^4$He and liquid $^3$He. The calculations were performed with Bose or Fermi hypernetted-chain techniques at the /0 level of accuracy [8] in which "elementary" or "bridge" diagrams are neglected. In other work of recent vintage, a path-integral Monte Carlo approach has been applied to obtain $\rho_{2h}(\boldsymbol{r}_1, \boldsymbol{r}_2, \boldsymbol{r}_1')$ for liquid $^4$He (with preliminary results reported in [40]). To the best of our knowledge, there has as yet been no quantitative microscopic treatment of $\rho_{2h}(\boldsymbol{r}_1, \boldsymbol{r}_2, \boldsymbol{r}_1')$ or $n(\mathbf{p}, \boldsymbol{Q})$ within the nuclear context, although computations based on stochastic procedures are in progress [41].

In this paper we shall exploit some of the technology developed by Ristig and Clark to gain computational insights into the structure of the generalized momentum distribution of uniform, infinite, symmetrical nuclear matter. Our study is largely patterned after that carried out for the one-body density matrix and single-particle momentum distribution by Flynn *et al.* [33], although the present considerations do not extend to Fermi hypernetted-chain (FHNC) resummation of higher-order clusters. The assumed state-independent Jastrow correlations $f(r)$ correspond to simple models of the ground state of nuclear matter involving repulsive cores at small interparticle separations [33]. We are interested in the qualitative behavior of $n(\boldsymbol{p}, \boldsymbol{Q})$ in different domains of the variables $\boldsymbol{p}$ and $\boldsymbol{Q}$. Since the computations are framed in the cluster-diagrammatic analysis of Ristig and Clark, the behavior of individual contributions may be readily interpreted in terms of the interplay of short-range correlations and exchange.

Such calculations may give a crude picture of $n(\boldsymbol{p}, \boldsymbol{Q})$ in medium-to-heavy nuclei. With this study as a basis (corrected, as necessary, by FHNC resummations), a better description may be obtained by implementing an appropriate local-density approximation, as has been done for the momentum distribution of finite nuclei in [42]. Future work should also address the problem of the inclusion of state-dependent correlations into the trial ground-state.

Section 2 recollects some necessary elements of the Ristig-Clark formalism and specifies *(i)* an approximation to $n(\boldsymbol{p}, \boldsymbol{Q})$ in term of the leading diagrams in a raw cluster expansion of this quantity [*lowest-order (LO) approximation*] and *(ii)* an approximation in terms of the structural for-

mula obtained in [30] by resummation of subseries of the raw expansion, irreducible components of this expression being evaluated to lowest cluster order [*lowest-order irreducible-cluster (LOIC) approximation*]. The models of nuclear matter adopted for our study are described in Sec. 3. Numerical results are reported and discussed in Sec. 4. We draw some general conclusions in Sec. 5 that anticipate the next steps toward realistic computation of the two-body density matrix in nuclear systems.

## 2. Cluster approximations

Our numerical calculations are based on the microscopic treatment of the half-diagonal two-body density $\rho_{2h}$ developed for Fermi fluids by Ristig and Clark [30] at the variational level of CBF theory [7, 8]. The analysis performed in [30] runs parallel to the more penetrating treatment of the Bose two-body density matrix formulated in [29] (with the distinction that general structural results may be derived in the Bose case without recourse to a Jastrow ansatz). These developments take advantage of techniques and results from earlier work on the one-body density matrix and momentum distribution of quantum fluids [43]. For the uniform Fermi system, the ground-state wave function is approximated by a trial wave function of Jastrow–Slater form

$$\Psi(1\cdots A) = \mathcal{N}^{-1}\prod_{i<j}^{A} f(r_{ij})\Phi(1\cdots A)\,, \tag{12}$$

where $\Phi$ is a Slater determinant of $A$ plane-wave orbitals filling the Fermi sea up to a wave number $k_{\mathrm{F}}$, $f(r_{ij})$ is the Jastrow two-body correlation function and $\mathcal{N}$ is a normalization constant. Considerations begin with the generalized momentum distribution $n(\mathbf{p}, Q)$ defined by Eq. (2). This quantity may be decomposed into a part that is present only for $Q = 0$, which is extensive in the particle number $A$, and a term present only for $Q \neq 0$ that is of order unity compared to $A$:

$$n(\boldsymbol{p}, \boldsymbol{Q}) = \delta_{Q0}(A-1)n(p) + (1-\delta_{Q0})\langle\Psi|N(\hat{\boldsymbol{p}}, \boldsymbol{Q})|\Psi\rangle\,. \tag{13}$$

The first term of this expression, henceforth denoted $n_0(\boldsymbol{p}, \boldsymbol{Q})$, contains no statistical or dynamical effects other than those embodied in the momentum distribution $n(p)$, and the remainder involves the expectation value of the non-self-adjoint operator

$$N(\hat{\boldsymbol{p}}, \boldsymbol{Q}) = \frac{\rho_Q a^\dagger_{\hat{\boldsymbol{p}}-\boldsymbol{Q}} a_{\hat{\boldsymbol{p}}} + a^\dagger_{\hat{\boldsymbol{p}}-\boldsymbol{Q}} a_{\hat{\boldsymbol{p}}}\rho_Q - a^\dagger_{\hat{\boldsymbol{p}}} a_{\hat{\boldsymbol{p}}} - a^\dagger_{\hat{\boldsymbol{p}}-\boldsymbol{Q}} a_{\hat{\boldsymbol{p}}-\boldsymbol{Q}}}{2}\,. \tag{14}$$

As shown in [30], the operator $N(\hat{p}, Q)$ may be written as a symmetric sum of two-body operators, allowing a factorized Iwamoto–Yamada (FIY) cluster expansion to be generated for the indicated expectation value using standard prescriptions [31, 8]. The individual terms of this expansion may be classified according to the number of orbital labels involved; as is customary, we will speak of "two-body," "three-body," ..., "n-body" cluster approximations when terms with more than two, more than three, ..., more than $n$ orbital indices are neglected. Evaluation is simplified by taking the thermodynamic limit, *i.e.*, $A \to \infty$ with $\rho$ held constant, thus restricting the treatment to a uniform infinite system. In this manner one arrives at a cluster series of the form

$$n(\boldsymbol{p}, \boldsymbol{Q}) = n_o(\boldsymbol{p}, \boldsymbol{Q}) + (1 - \delta_{Q0})\left[n_{(2)}(\boldsymbol{p}, \boldsymbol{Q}) + n_{(3)}(\boldsymbol{p}, \boldsymbol{Q}) + \cdots\right], \qquad (15)$$

wherein the *subscript* $(i)$ on an addend counts the number of "bodies" involved. [We note that the corresponding expansion in Eq. (12) of [30] should be corrected by replacing the first term on the right, appearing as $n_F(\boldsymbol{p}, \boldsymbol{Q})$, by $n_o(\boldsymbol{p}, \boldsymbol{Q})$ as defined above and in Eq. (4) of that paper.] Examination of the terms in the series (15) reveals that $n(\boldsymbol{p}, \boldsymbol{Q})$ is a *reducible* quantity, in the sense of containing factorizable contributions — *i.e.*, it has the structure of a sum of products of Ursell–Mayer cluster diagrams [8, 43]. However, with appropriate graphical resummations the generalized momentum distribution may be succinctly expressed in terms of a small number of quantities, each defined by a cluster expansion in *irreducible* (non-factorable) diagrams. Fermi hypernetted-chain procedures have been devised for evaluation of these irreducible quantities by solution of coupled integral equations. The structural expression derived by Ristig and Clark reads

$$\begin{aligned} n(\boldsymbol{p}, \boldsymbol{Q}) &= (A-1)\delta_{Q0} n(p) \\ &+ (1 - \delta_{Q0}) F_{dd}(Q)[n(p) + n(|\boldsymbol{p} - \boldsymbol{Q}|)] \\ &+ (1 - \delta_{Q0}) F_{de}(Q)[n_{Dl}(p) + n_{Dl}(|\boldsymbol{p} - \boldsymbol{Q}|)] \\ &- n(1 - \delta_{Q0})[\Theta(k_{\mathrm{F}} - p) - F_{cc}(p)][\Theta(k_{\mathrm{F}} - |\boldsymbol{p} - \boldsymbol{Q}|) - F_{cc}(|\boldsymbol{p} - \boldsymbol{Q}|)] \\ &+ (1 - \delta_{Q0}) n^{(2)'}(\boldsymbol{p}, \boldsymbol{Q}) + (1 - \delta_{Q0}) n^{(3)'}(\boldsymbol{p}, \boldsymbol{Q}) . \end{aligned} \qquad (16)$$

[This expression corresponds to Eq. (42) of [30]; however the strength factor $n_o$ appearing in the fourth term of Eq. (42) has been renamed as $n$ (cf. [43, 33]) to avoid confusion with the first term of Eq. (13) or Eq. (5) above. We note incidentally that a square bracket is missing from the end of the first line of Eq. (42).]

We must refer the reader to [30] for detailed definitions of the two-point form factors $F_{dd}(Q)$, $F_{de}(Q)$, $F_{cc}(p)$ and $F_{cc}(|\boldsymbol{p} - \boldsymbol{Q}|)$ in terms of series of irreducible cluster diagrams, for specification of the modified single-particle

momentum distribution $n_{Dl}(p)$ and for characterization of the more complicated, three-point quantities $n^{(2)'}(\boldsymbol{p},\boldsymbol{Q})$ and $n^{(3)'}(\boldsymbol{p},\boldsymbol{Q})$. The designations "two-point" and "three-point" refer to the configuration-space functions whose Fourier transforms yield $F_{dd}(Q)$, $n^{(2)'}(\boldsymbol{p},\boldsymbol{Q})$, *etc.* In particular, we have $F_{xy}(k) = \rho \int F_{xy}(r)\mathrm{e}^{i\boldsymbol{k}\cdot\boldsymbol{r}}d\boldsymbol{r}$ (where $xy = dd$, $de$, or $cc$), and $F_{xy}(r)$ is by construction a two-point object. A structural formula for the ordinary momentum distribution function $n(p)$ corresponding to the wave function (12) has been given in [43], where (among many other manipulations) the series defining the strength factor $n = \exp[-\mathcal{Q}(0)]$ is re-summed in terms of an irreducible-diagram sum $\mathcal{Q}(r)$. It should be remarked that the explicit result (16) is predicated on satisfaction of the sequential relation (11), which, in the present context, is equivalent to the condition [30]

$$2F_{dd}(0)n(p) + 2F_{de}(0)n_{Dl}(p) - n[\Theta(k_{\mathrm{F}} - p) - F_{cc}(p)]^2 + n^{(2)'}(\boldsymbol{p},0) + n^{(3)'}(\boldsymbol{p},0) = -n(p)\,. \qquad (17)$$

There exist Fermi-hypernetted chain algorithms for quantitative determination of all of the irreducible ingredients of (16), including the various form factors $F_{xy}(k)$ as well as the irreducible components of the single-particle momentum distributions $n(p)$ and $n_{Dl}(p)$, of the strength factor $n$ and of the three-point quantities $n^{(2)'}(\boldsymbol{p},\boldsymbol{Q})$ and $n^{(3)'}(\boldsymbol{p},\boldsymbol{Q})$. Alternatively, one may resort to stepwise evaluation of the terms in the cluster expansions of these ingredients (see below).

The renormalized expression (16) serves to clarify the physics contained in the generalized momentum distribution, by collecting into separate terms the contributions from various virtual scattering processes. The first term reproduces the trivial result [*viz.* Eq. (4)] for dynamically and statistically uncorrelated particles, with the important qualification that the momentum distribution function of the fully correlated Fermi system is to be inserted. The correlations prevailing in the interacting fluid permit the scattering of a fermion from orbital $\hat{\boldsymbol{p}}$ to another orbital $\hat{\boldsymbol{p}} - \boldsymbol{Q}$, with the intervention of a phonon to conserve momentum. This process and the corresponding time-reversed mechanism are represented by the second term in (16), involving the direct form factor $F_{dd}(Q)$. The associated exchange scattering effects are given by the third term, which is proportional to the exchange form factor $F_{de}(Q)$. The fourth term incorporates the kinematic effect of the Pauli exclusion principle seen in Eq. (5), but corrected by the dynamical (Jastrow) correlations. (The $F_{cc}$ corrections account for the population of states outside the Fermi sea by the interactions. The dynamical correlations also produce an overall quenching of the Pauli kinematic effect through the strength factor $n$ ($0 \leq n \leq 1$), which accounts for the depletion of the Fermi sea.) The last two terms of (16) describes virtual processes of more complicated nature, which serve to correct those already described.

From either the raw cluster expansion (15) or the re-summed structural expression (16) we observe that at $Q = 0$ the generalized momentum distribution function just reproduces the single-particle momentum distribution $n(p)$, with the large factor $A - 1$. Accordingly, our numerical considerations will focus on the nontrivial addend that enters when $Q \neq 0$ (this portion being of order unity compared to $A$).

We shall explore two simple approximation schemes for the evaluation of $n(\mathbf{p}, Q)$ within the theoretical framework outlined above.

*Lowest-Cluster-Order Approximation (LO).* The first procedure involves straightforward implementation of the cluster expansion (15). The series in square brackets is truncated at the leading, two-body cluster order; thus we retain only the addend $n_{(2)}$, which, in detail, consists of a sum of seven two-body cluster contributions:

$$n_{(2)}(p, Q) = \sum_{i=1}^{7} n_{(2)}^{[i]}(p, Q) . \tag{18}$$

The Ursell–Mayer diagrams that depict the individual terms are shown in Fig. 2. (For an explanation of the relevant graphical conventions, see the Appendix of [30]. Strictly, this approximation amounts to retaining only the two-orbital portion of $n(p, Q) - n_o(p, Q)$ expanded via the factorized Iwamoto-Yamada algorithm [30,31].) The corresponding analytic contributions to the two-body cluster approximation $\rho_{2h(2)}(r_1, r_2, r_1')$ for the half-diagonal two-body density matrix are (in the same order as in Fig. 2 and Eq. (18)):

$$\begin{aligned}
& l(k_F r_{11'})\zeta(r_{12}) , \\
& l(k_F r_{11'})\zeta(r_{1'2}) , \\
& l(k_F r_{11'})\zeta(r_{1'2})\zeta(r_{12}) , \\
& -\nu^{-1} l(k_F r_{12}) l(k_F r_{1'2}) , \\
& -\nu^{-1} l(k_F r_{12})\zeta(r_{1'2}) l(k_F r_{1'2}) , \\
& -\nu^{-1} l(k_F r_{12})\zeta(r_{12}) l(k_F r_{1'2}) , \\
& -\nu^{-1} l(k_F r_{12})\zeta(r_{12}) l(k_F r_{1'2})\zeta(r_{1'2}) .
\end{aligned}$$

Here, $l(x) = 3x^{-3}(\sin x - x\cos x)$ is the Slater exchange function and $\zeta(r) = f(r) - 1$ is a dynamical correlation bond. We use the notation $r_{12} = |r_1 - r_2|$, $r_{11'} = |r_1 - r_1'|$ and $r_{1'2} = |r_1' - r_2|$.

The LO approximation $n_{\mathrm{LO}}(p, Q)$ so defined is evidently equivalent to taking the two-body part of the component of (16) proportional to $(1 - \delta_{Q0})$. Upon detailed comparison it is seen that the cluster terms $n_{(2)}^{[1]}$ and $n_{(2)}^{[2]}$ ap-

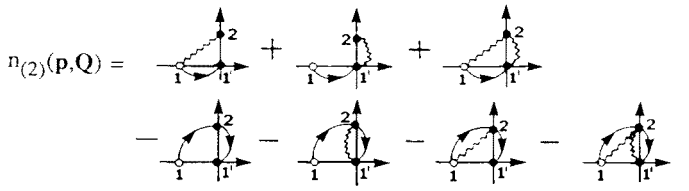


Fig. 2. Diagrammatic representation of the two-body cluster contributions $n_{(2)}^{[i]}(\boldsymbol{p}, \boldsymbol{Q})$ to the expansion (18) of the generalized momentum distribution function, drawn in the order $i = 1, \ldots, 7$ [30]. Wavy lines represent dynamical-bond factors $\zeta(r_{ij})$, curved oriented lines denote Slater exchange factors $l(k_{\mathrm{F}} r_{ij})$, and straight oriented lines stand for plane waves $\exp(i\boldsymbol{k} \cdot \boldsymbol{r}_{ij})$ of momentum $\boldsymbol{k} = \boldsymbol{p}$ (horizontal) or $\boldsymbol{k} = \boldsymbol{Q}$ (vertical).

pearing in Eq. (18) and Fig. 2 derive from the second term of the decomposition (16), representing the scattering of a nucleon from a plane-wave state of momentum $\boldsymbol{p}$ to another plane-wave orbital of momentum $\boldsymbol{p} - \boldsymbol{Q}$ with the exchange of a momentum-conserving phonon (plus the time-reversed counterpart of this process). To the order considered, the third term in (16) does not contribute. The cluster terms $n_{(2)}^{[i]}$ with $i = 4, \ldots, 7$ belong to the fourth term of (16), which describes the scattering of Pauli-correlated nucleons, modified by dynamical effects associated with the depletion of the Fermi sea and population of states above the Fermi sea. Of course, the piece $n_{(2)}^{[4]}$ is identical, for $Q \neq 0$, to the generalized momentum distribution (5) of the ideal Fermi gas. Finally, the term $n_{(2)}^{[3]}$ is the leading cluster contribution to the addend $n^{(2)'}$ of (16) that incorporates some of the higher-order virtual processes.

It may easily be verified that the approximation $n_{\mathrm{LO}}(\boldsymbol{p}, \boldsymbol{Q})$ conserves the following properties of the exact generalized momentum distribution: *(i)* time-reversal invariance, *(ii)* the $\boldsymbol{p}$ sum rule of Eq. (8) and *(iii)* the $\boldsymbol{Q}$ sum rule of Eq. (9). (In verifying (8) and (9), one must naturally adopt the two-body cluster approximation $g_{\mathrm{LO}}(r) = f^2(r)[1 - l^2(k_{\mathrm{F}} r)/\nu]$ to the radial distribution function.) On the other hand, $n_{\mathrm{LO}}(\boldsymbol{p}, \boldsymbol{Q})$ violates the sequential condition (11) (or equivalently (17)) when we extend the implementation of the two-body cluster approximation to $Q \neq 0$ and also apply it to the single-particle momentum distribution $n(p)$.

*Lowest-Order-Irreducible-Cluster Approximation (LOIC).* The second calculational procedure goes beyond simple approximation of $n(\boldsymbol{p}, \boldsymbol{Q})$ to lowest cluster order in the expansion (15), yet it still determines the generalized momentum distribution in terms of quantities evaluated in lowest cluster order. Instead of truncating the raw cluster series (15) at two-body order,

we work with the re-summed form of the expansion given by Eq. (16). This renormalized expansion captures the sum-of-products structure of $n(\boldsymbol{p},\boldsymbol{Q})$, expressing it as a function of certain irreducible-diagram sums. The general prescription we adopt – LOIC – is to evaluate these irreducible-diagram sums in lowest (two-body) cluster order. Specifically, we make the following approximations to the irreducible two-point quantities $F_{xy}(r)$ that determine the form factors $F_{dd}(Q)$, $F_{de}(Q)$, $F_{cc}(p)$ and $F_{cc}(|\boldsymbol{p}-\boldsymbol{Q}|)$ (see Fig. 13 of [30]): $F_{dd}(r)=\zeta(r)$, $F_{de}(r)=0$ and $F_{cc}(r)=-\zeta(r)l(k_{\rm F}r)$.

The single-particle momentum distribution $n(k)$ (needed for $k=p$ and $|\boldsymbol{p}-\boldsymbol{Q}|$) is itself a diagrammatically reducible quantity, itself expressible in renormalized form in terms of irreducible-cluster sums [43]. Accordingly, for this quantity we invoke the lowest-order irreducible-cluster approximation $n_{\rm LOIC}(k)$ as defined and studied by Flynn *et al.* [33]. The treatment of the modified momentum distribution $n_{Dl}(k)$ appearing in the third term of (16) is moot because the factor $F_{de}(Q)$, which has no two-body part, is neglected. The strength factor $n=\exp[\mathcal{Q}(0)]$ is determined by truncating the expansion for $\mathcal{Q}(r=0)$ at two-body order. Thus we set $n=\exp[-\kappa_{\rm dir}]$ with $\kappa_{\rm dir}\equiv\rho\int\zeta^2(r)d\boldsymbol{r}$.

We deviate from the strict LOIC prescription in the disposition of the last two terms of Eq. (16). The separable three-point configuration-space kernel defining the addend $n^{(2)'}(\boldsymbol{p},\boldsymbol{Q})$ of (16) is approximated by the leading diagram in the raw cluster expansion of the first term of Eq. (38) in [30] (noting that the $Q$ subscripts in that equation are superfluous). Explicitly, this kernel is taken as $K(\boldsymbol{r}_1,\boldsymbol{r}_2,\boldsymbol{r}_1')=\rho^2 l(k_{\rm F}r_{11'})\zeta(r_{12})\zeta(r_{1'2})$. The more complicated three-point quantity $n^{(3)'}(\boldsymbol{p},\boldsymbol{Q})$ is set equal to zero.

The approximation so defined is called LOIC1, in anticipation of improved approximations which include additional leading contributions to the irreducible-diagram sums.

To compare LOIC1 and LO procedures in the context of expression (16), we may observe that the addends $n^{[1]}_{(2)}$ and $n^{[2]}_{(2)}$ of the cluster decomposition (18) correspond to the second term of (16), $n^{[3]}_{(2)}$ is contained in the fifth, and $n^{[4]}_{(2)}$, $n^{[5]}_{(2)}$, $n^{[6]}_{(2)}$ and $n^{[7]}_{(2)}$ are all generated by the fourth. The two approximations, LOIC1 and LO, coincide in their treatment of the form factors $F_{dd}$, $F_{de}$ and $F_{cc}$. They likewise coincide in their neglect of $n^{(3)'}(\boldsymbol{p},\boldsymbol{Q})$ and in their approximation of $n^{(2)'}(\boldsymbol{p},\boldsymbol{Q})$ by the third diagram of Fig. 2, *i.e.* by $n^{[3]}_{(2)}$. Differences arise (for $Q\neq 0$) only from two sources:

*(i)* In the LO prescription, step functions $\Theta(k_{\rm F}-k)$ corresponding to the ideal Fermi gas are used in place of the momentum-distribution factors $n(k)$ appearing in the second term on the right-hand side of

(16), whereas $n_{\mathrm{LOIC}}(k)$ factors are inserted in implementing the LOIC1 scheme.

*(ii)* Similarly, the strength factor $n$ in the fourth term of (16) is replaced by unity in the LO treatment, but is approximated by $\exp(-\kappa_{\mathrm{dir}})$ in LOIC1.

The LOIC1 approximation maintains time-reversal invariance and again satisfies the $\boldsymbol{p}$ and $\boldsymbol{Q}$ sum rules (for consistently defined $g_{\mathrm{LOIC1}}(r)$ and $S_{\mathrm{LOIC1}}(Q)$). In the examples treated numerically, the violation of the sequential relation by the LOIC1 procedure is somewhat less severe than occurs in the LO approximation (see Sec. 4). It should be pointed out that failure of the sequential relation has no direct effect on the evaluation of $n(\boldsymbol{p}, \boldsymbol{Q})$ away from $Q = 0$.

## 3. Models of nuclear matter

We have considered simple models of the ground state of symmetrical nuclear matter near its saturation density. These models are intended primarily to capture the essential aspects of the short-range repulsive correlations that exist in nuclei; they will – at best – only reflect the effects of the intermediate and longer-range components of the nuclear force in a qualitative manner. The models are specified through the state-independent two-body Jastrow correlation function $f(r)$ of Eq. (12) and the Fermi wave number $k_{\mathrm{F}}$.

*Monte Carlo Model (MC).* One choice for $f(r)$, with associated density $\rho = 0.182\ \mathrm{fm}^{-3}$ ($k_{\mathrm{F}} = 1.392\ \mathrm{fm}^{-1}$), is taken from the variational Monte Carlo study of Ceperley, Chester and Kalos [44]:

$$f(r) = \exp[-c_1 \mathrm{e}^{-c_2 r} \frac{(1 - \mathrm{e}^{-r/c_3})}{r}] \qquad (\mathrm{MC}). \tag{19}$$

The parameters $c_1 = 1.7$ fm, $c_2 = 1.6\ \mathrm{fm}^{-1}$ and $c_3 = 0.1$ fm were determined [44] by minimization of the ground-state energy expectation value of symmetrical nuclear matter with respect to the corresponding Jastrow–Slater trial state. The assumed interaction is the $v_2$ "homework potential" [8, 45], given by the central part of the Reid soft-core interaction in the $^3\mathrm{S}_1$–$^3\mathrm{D}_1$ channel, which is considered to act in all partial waves. This central, state-independent potential choice has been employed in quite a number of exploratory studies of nuclear matter (see *e.g.* [8, 33, 44–47]). It has a repulsive core that is relatively stiff compared to those of some supposedly realistic nucleon-nucleon interactions.

*Gaussian Models (G1 and G2).* We have also investigated two other models based on a Jastrow two-body correlation function with Gaussian deviation from unity:

$$f(r) = 1 - \exp[-\beta^2 r^2] \qquad (\mathrm{G1},\ \mathrm{G2}). \tag{20}$$

These models are not connected with any known nucleon-nucleon interactions, but would clearly be associated with potentials having soft repulsive cores. They have the convenient feature of permitting analytic evaluation of the integrals that enter the approximation $n_{\mathrm{LO}}(p,Q)$. Model G1 refers to a density $\rho = 0.1589$ fm$^{-3}$ ($k_{\mathrm{F}} = 1.33$ fm$^{-1}$). The parameter value $\beta = 1.1$ fm$^{-1}$ completing the specification of G1 was determined [42] by fitting a low-order calculation of the momentum distribution $n(p)$ of nuclear matter at this density to the result of a correlated-basis-functions calculation [34] of $n(p)$ for a realistic two-nucleon interaction. Model G2, with $\beta = 1.478$ fm$^{-1}$, refers to $\rho = 0.182$ fm$^{-3}$ ($k_{\mathrm{F}} = 1.392$ fm$^{-1}$). It has been used in the work of Flynn *et al.* [33], which tested various methods for numerical computation of $n(p)$ for a Jastrow–Slater wave function (12). The methods considered in [33] include the LOC (lowest-order conserving), LOIC (lowest-order irreducible-cluster), FHNC (Fermi-hypernetted chain) and MC (variational Monte Carlo) procedures.

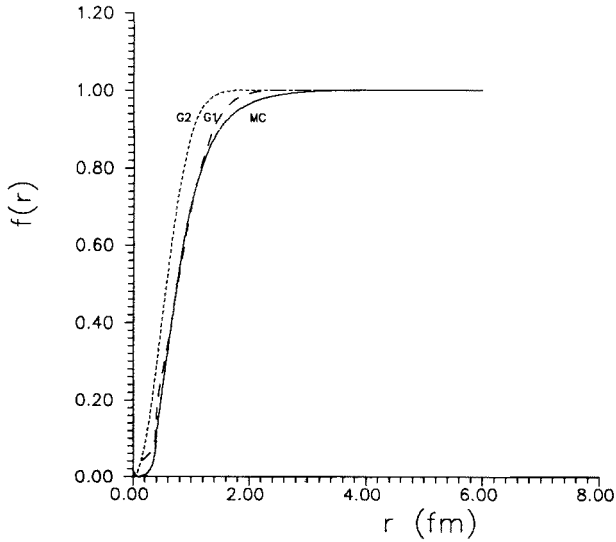


Fig. 3. Correlation functions $f(r)$ of the three models of symmetrical nuclear matter designated as MC, G1 and G2 (see text).

Their qualitative nature notwithstanding, the models defined above will provide reasonable surrogates for realistic nuclear matter, allowing us to study effects of different aspects of the state-independent geometrical correlations on the two-body density matrix. The correlation functions $f(r)$ characterizing the three models are compared in Fig. 3. While quite similar in appearance, they nevertheless show significant differences in behavior both in the core region and at medium distances. A commonly invoked

measure of the overall strength of the dynamical correlations is the wound parameter $\kappa_{\rm dir}$ introduced in Sec. 2 in approximating the strength factor $n$. This quantity estimates the effectiveness of the correlations in depleting the Fermi sea; indeed, the logarithm of the residue at the quasiparticle pole, as given in leading cluster order of variational theory [43], is just $-\kappa_{\rm dir}$. The respective values of the wound parameter for models MC, G1 and G2 are $\kappa_{\rm dir} = 0.297$, 0.237 and 0.111. Accordingly, the models chosen for investigation span a range from relatively strong to relatively weak correlations.

## 4. Numerical results and their assessment

Selected results from numerical calculations of $n(\boldsymbol{p},\boldsymbol{Q})$ based on the nuclear-matter models MC, G1 and G2 are displayed in Figs. 4-12. We have considered the respective ranges $[0, 3k_{\rm F}]$ and $[0, 5k_{\rm F}]$ in the magnitudes of the momentum variables $\boldsymbol{p}$ and $\boldsymbol{Q}$, keeping $Q > 0$ unless otherwise indicated. *Results in LO Approximation.* As a basis for further discussion, let us first examine results of the straightforward lowest-cluster-order evaluation for the MC model, in the special case that $\boldsymbol{p}$ and $\boldsymbol{Q}$ are parallel (*i.e.* $\boldsymbol{Q} = Q\boldsymbol{p}/p$). Two views of $n_{\rm LO}(\boldsymbol{p},\boldsymbol{Q})$ for this case are shown in Figs. 4 and 5. For the noninteracting Fermi gas, $n(\boldsymbol{p},\boldsymbol{Q})$ (for $Q \neq 0$) coincides with $n^{[4]}_{(2)}$ and (from Eq. (5)) is simply $-1$ for $p \leq k_{\rm F}$ and $0 \leq Q \leq p + k_{\rm F}$, and zero otherwise. Consider a fixed $p \leq k_{\rm F}$ and let $Q$ vary. In the two plots the full $n_{\rm LO}(\boldsymbol{p}, Q\boldsymbol{p}/p) = n_{(2)}(\boldsymbol{p},\boldsymbol{Q})$ is seen to increase monotonically with $Q$ for $Q \leq p + k_{\rm F}$, starting from substantial negative values at small $Q$. At $Q = p + k_{\rm F}$, this function exhibits a steep rise toward zero. For values of $Q$ in the range $0 \leq Q \leq p + k_{\rm F}$, the terms $n^{[1]}_{(2)}$, $n^{[2]}_{(2)}$ and $n^{[4]}_{(2)}$ are comparable in size and make the contributions to $n_{\rm LO}(\boldsymbol{p}, Q\boldsymbol{p}/p)$ of largest magnitude, the terms $n^{[5]}_{(2)}$, $n^{[6]}_{(2)}$ and $n^{[3]}_{(2)}$ are of smaller size, and the remaining term $n^{[7]}_{(2)}$ is the least consequential. The deviation of $n_{\rm LO}(\boldsymbol{p}, Q\boldsymbol{p}/p)$ from zero in the region $Q > p + k_{\rm F}$ is attributable entirely to the presence of dynamical correlations; of the four nonvanishing terms, $n^{[2]}_{(2)}$, $n^{[5]}_{(2)}$ and $n^{[3]}_{(2)}$ are of comparable size, while $n^{[7]}_{(2)}$ is considerably smaller in magnitude. Dynamical correlations are also responsible for the nonzero values of $n(\boldsymbol{p},\boldsymbol{Q})$ seen at $p > k_{\rm F}$. In this $p$ range, and for $Q$ satisfying $|p - k_{\rm F}| \leq Q \leq p + k_{\rm F}$, it is $n^{[1]}_{(2)}$ and next $n^{[6]}_{(2)}$ that give the leading contributions, followed by $n^{[3]}_{(2)}$ and $n^{[7]}_{(2)}$. The latter two terms also contribute in the region $Q > p + k_{\rm F}$. Our findings for the relative sizes of the individual contributions to $n_{\rm LO}(\boldsymbol{p},\boldsymbol{Q})$ are generally understandable in terms of the number of correlation lines (the wavy lines

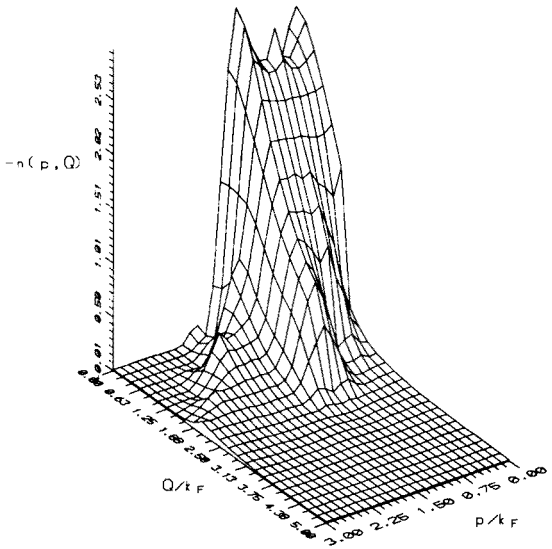


Fig. 4. Lowest-order generalized momentum distribution $n_{\rm LO}(p, Q)$ as a function of $p$ and $Q$ for $p$ parallel to $Q$ (and $Q \neq 0$), calculated with the MC correlation function of Ref. [44] at density $\rho = 0.182$ fm$^{-3}$.

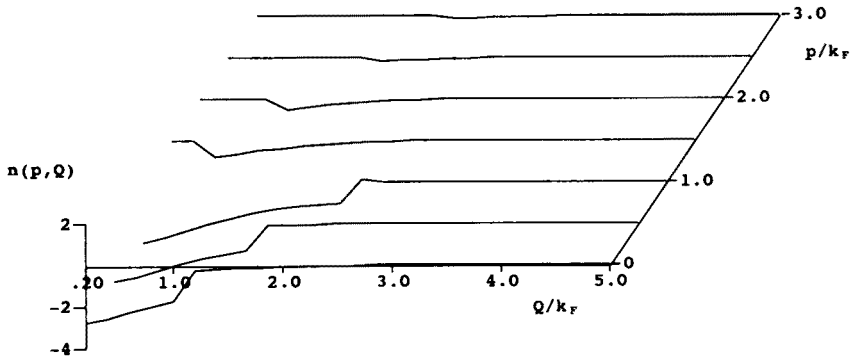


Fig. 5. A different view of the data of Fig. 4.

representing $\zeta$ factors) involved in the corresponding diagrams, as well as the associated factors in the density $\rho$ and the inverse degeneracy $\nu^{-1} = 1/4$.

Fig. 6 provides numerical data on the variation of $n_{\rm LO}(p, Q)$ with the angle $\theta_{pQ}$ between $p$ and $Q$, in the special case $p = k_{\rm F}$. For all four choices of $Q$, it would seem that $n_{\rm LO}(p, Q)$ attains its minimum value at or very near $\theta_{pQ} = 0$, *i.e.*, when $p$ and $Q$ are parallel. In the examples with $Q \leq 2k_{\rm F}$ (*i.e.*, for which there would be a nonvanishing result with the dynamical correlations switched off), the approximated function rises rather steeply somewhere between $\theta_{pQ} = 0$ and $\theta_{pQ} = \pi/2$, and then appears to flatten

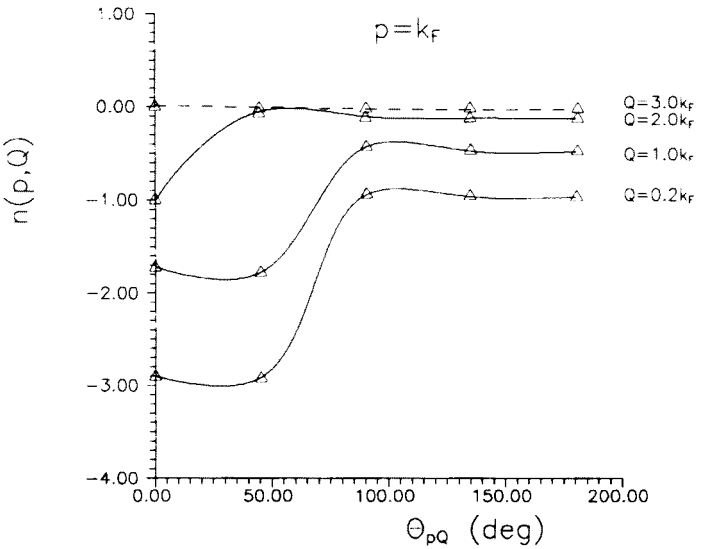


Fig. 6. Lowest-order generalized momentum distribution $n_{\mathrm{LO}}(p, Q)$ as a function of the angle $\theta_{pQ}$ between $p$ and $Q$, for $p = k_{\mathrm{F}}$ and the indicated $Q$ values. The MC correlation function [44] and corresponding density $\rho = 0.182$ fm$^{-3}$ were assumed. (Numerical results are plotted as small triangles; the curves have been drawn merely to guide the eye.)

out. Broadly similar behavior has been observed at other values of $p$.

Figs. 7-9 exemplify the dependence of the results on the choice of correlation function (and density), for $\theta_{pQ} = 0$ and three characteristic values of $p$, namely 0, $k_{\mathrm{F}}$ and $2k_{\mathrm{F}}$. Although the predictions for the three models MC, G1 and G2 are qualitatively similar, there are conspicuous quantitative differences at small and intermediate $Q$ values. One observation (intended as a general statement but subject to exception) is that the departure of $n_{\mathrm{LO}}$ from the result (5) for the ideal Fermi gas is found to be larger for larger wound parameter $\kappa_{\mathrm{dir}}$. An exception that warrants attention is the behavior of the MC result just below $Q = p + k_{\mathrm{F}}$ (notably in Figs. 8 and 7): one sees a (negative) "depletion" relative to the results for the other two models. We may further remark at this point that the violation of the sequential relation is also found to increase with the size of $\kappa_{\mathrm{dir}}$.

The predictions of the three models of nuclear matter appear to merge at large $Q$ (*i.e.* beyond $Q = p + k_{\mathrm{F}}$). On the other hand, the dynamical contributions outside the $Q$ range $\max\{0, p - k_{\mathrm{F}}\} \leq Q \leq p + k_{\mathrm{F}}$ conditionally accessible to the noninteracting Fermi gas are of relatively modest size (compared to unity). This finding contrasts with the substantial dynamical

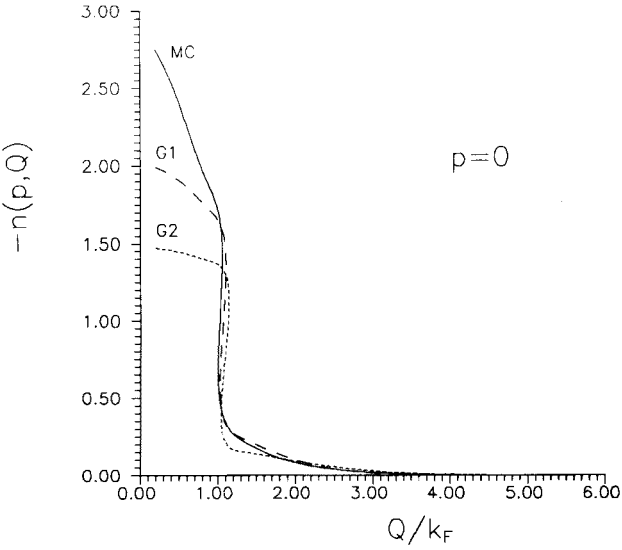


Fig. 7. Lowest-order generalized momentum distribution $n_{\mathrm{LO}}(p, Q)$ as a function of $Q(>0)$, at $p = 0$, for the three models MC, G1 and G2. The corresponding result for the ideal Fermi gas is $-1$ for $Q/k_{\mathrm{F}} \leq 1$ and zero otherwise.

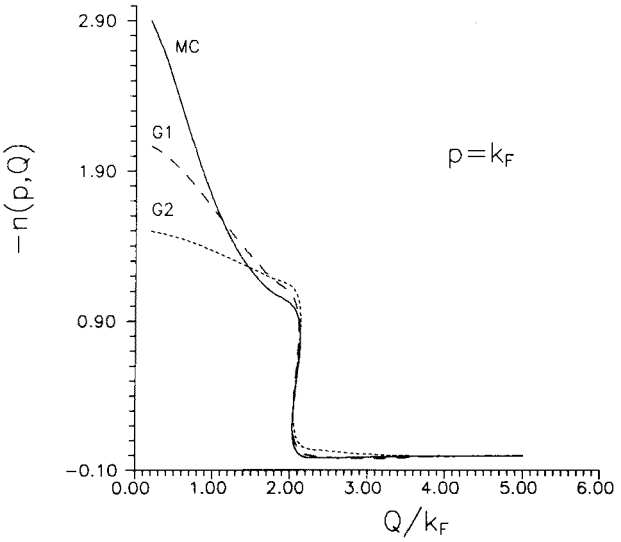


Fig. 8. The lowest-order generalized momentum distribution $n_{\mathrm{LO}}(p, Qp/p)$ as a function of $Q(>0)$ for $Q\|p$, at $p = k_{\mathrm{F}}$, for the three models MC, G1 and G2. The corresponding result for the ideal Fermi gas is $-1$ for $Q/k_{\mathrm{F}} \leq 2$ and zero otherwise.

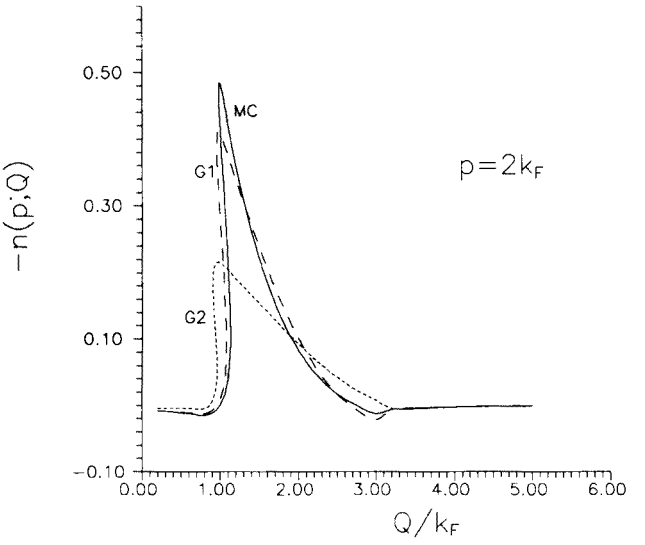


Fig. 9. As in Fig. 8, but for $p = 2k_F$. The corresponding result for the ideal Fermi gas is zero. Note the difference in scale relative to Fig. 8.

effects evident for low $Q$ at $p = 0$ and $p = k_F$ (Figs. 7-8). In the case $p = 2k_F$ (Fig. 9), where statistical correlations alone would make no contribution, we observe significant departures from the Fermi-gas prediction, at the level of 10-50%, depending on the model assumed. The deviations are concentrated in the $Q$ range $[p - k_F, p + k_F] = [k_F, 3k_F]$. These features may be traced to the presence of Fermi-gas step functions ($\Theta(k_F - p)$ and/or $\Theta(k_F - |\boldsymbol{p} - \boldsymbol{Q}|)$) in the more important addends of Eq. (18).

Silver [39] has proposed simple approximation $n(\boldsymbol{p}, \boldsymbol{Q}) = n(p)[S(Q) - 1]$ for the generalized momentum distribution at $Q \neq 0$, in terms of the single-particle momentum distribution $n(p)$ and the static structure function $S(Q)$. We have investigated this ansatz using inputs $n(p)$ and $S(Q)$ calculated for the MC model in FHNC/0 approximation. The results are substantially smaller in magnitude than we have found with the LO approximation procedure, in the "Fermi-gas" regime defined by nonvanishing $\Theta(k_F - p)\Theta(k_F - |\boldsymbol{p} - \boldsymbol{Q}|)$. It is to be recalled [30] that Silver's formula breaks time-reversal invariance and also misses the Pauli kinematic effect represented by the fourth term of (16).

*Results in LOIC1 Approximation.* Our numerical findings with the LOIC1 procedure are summarized in Figs. 10 and 11, while Fig. 12 compares selected results from LO and LOIC1 calculations. First, consider the relative strengths of individual contributions to the LOIC1 estimate of $n(\boldsymbol{p}, \boldsymbol{Q})$ in the reference case having $\boldsymbol{Q}$ parallel to $\boldsymbol{p}$ ($\Theta_{\boldsymbol{pQ}} = 0$). The individual contributions in question include the "dressed" counterparts of the LO addends

$n^{[1]}_{(2)}$ and $n^{[2]}_{(2)}$ of (18), which are dressed by replacing the factors $\Theta(k_F - k)$ by $n_{\rm LOIC}(k)$, and of the sum of LO addends $n^{[4]}_{(2)}$ through $n^{[7]}_{(2)}$, which are dressed by attaching the approximate strength factor $n_{\rm LOIC} = \exp(-\kappa_{\rm dir})$. It will be convenient to denote the dressed quantities by the same symbols as used in the LO calculation, save that the subscript (2) is omitted. The dressed sum $n^{[4]} + n^{[5]} + n^{[6]} + n^{[7]}$, which we abbreviate as $n^{[4-7]}$, evidently constitutes the LOIC1 approximation to the Pauli kinematic term of (16) (the fourth term). The remaining contribution to the LOIC1 estimate is of course identical with the addend $n^{[3]}_{(2)}$ of the LO prescription. With $p$ fixed at $k_F$, and $Q$ below $2k_F$, the most important contributions are $n^{[4-7]}$, $n^{[2]}$ and $n^{[1]}$, the term $n^{[3]}_{(2)} = n^{[3]}$ being of lesser magnitude. As $Q$ increases through $2k_F$ there is an abrupt change of $n_{\rm LOIC1}(p, Q)$ (the expected upward shift toward zero), and for $Q > 2k_F$, the contributions $n^{[4-7]} \approx n^{[2]}$ have the largest magnitudes, then $n^{[3]}$ and then $n^{[1]}$. Changing $p$ to $2k_F$, the descending order of dominance, for $k_F < Q < p + k_F = 3k_F$, is $n^{[1]}$, then $|n^{[3]}| \approx |n^{[4-7]}|$ and then $n^{[2]}$. Near $Q = k_F$ the approximate $n(p, Q)$ shows an abrupt drop from near-zero values, followed by a gradual rise toward zero as $Q$ increases through the range $k_F < Q < 3k_F$. This general pattern holds for all three models of nuclear matter.

Turning to a comparison of results for the different models, we find much the same picture as in the LO calculation, particularly with respect to the deviations from Fermi-gas behavior and their dependence on the wound parameter $\kappa_{\rm dir}$. It is interesting and perhaps significant that the "depletion" effect just below $Q = 2k_F$ noted in the LO result at $p = k_F$ for the MC model – which has the largest $\kappa_{\rm dir}$ of the three models – has now become an actual (negative) depletion relative to the Fermi-gas result (see Fig. 10).

Finally, the differences between the results from the two calculational schemes, LO and LOIC1, should be assayed. Attention is restricted to models MC and G2, which have the largest and smallest wound parameters, respectively. Let $\Delta n(p, Q)$ be the relative discrepancy between the two evaluations of the generalized momentum distribution, determined by $|[n_{\rm LO}(p, Q) - n_{\rm LOIC1}(p, Q)]/n_{\rm LO}(p, Q)|$ and quoted as a percentage. First consider the case $p = k_F$ (*cf.* Fig. 12). For $Q < 2k_F$, we find (very roughly) $\Delta n \sim 20\%$ (MC) and $\sim 10\%$ (G2), the discrepancies decreasing slightly with increasing $Q$. The higher-order contributions present in LOIC1 (but not in LO) have a net positive effect and thus act to reduce the departure from the Fermi-gas limit. For $Q > 2k_F$, we again find $\Delta n \sim 20\%$ in the MC model, but the net contribution of the higher-order terms is now negative. For the G2 model the small numerical magnitudes of the relevant quantities

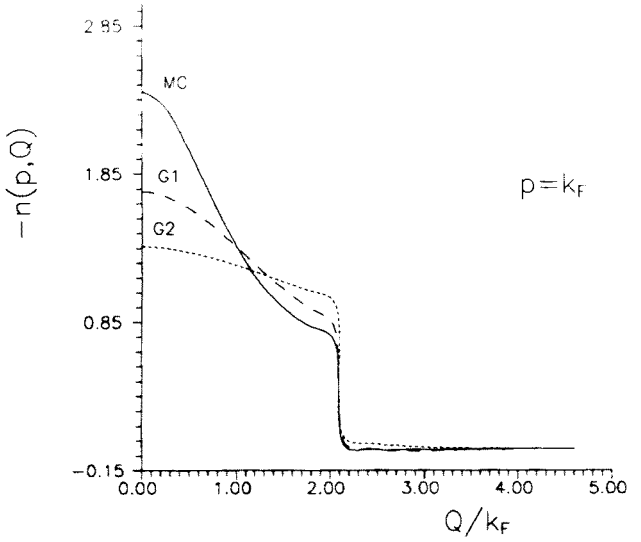


Fig. 10. Lowest-order irreducible-cluster approximation $n_{\mathrm{LOIC1}}(\boldsymbol{p}, Q\boldsymbol{p}/p)$ to the generalized momentum distribution, as a function of $Q(>0)$ for $\boldsymbol{Q}\|\boldsymbol{p}$, at $p = k_{\mathrm{F}}$, for the three models MC, G1 and G2.

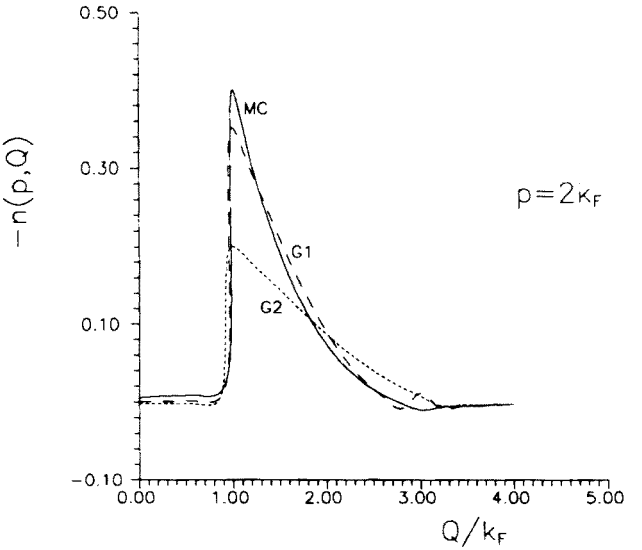


Fig. 11. As in Fig. 10, but for $p = 2k_{\mathrm{F}}$.

and differences hinder a useful comparison of the two procedures. In the case $p = 2k_{\mathrm{F}}$, the estimated values of $n(\boldsymbol{p}, \boldsymbol{Q})$ for $Q < k_{\mathrm{F}}$ or $Q > 3k_{\mathrm{F}}$ are also too small in magnitude for useful comments to be made, for either MC or G2. However, in the range $k_{\mathrm{F}} < Q < 3k_{\mathrm{F}}$, the discrepancy $\Delta n$ runs from

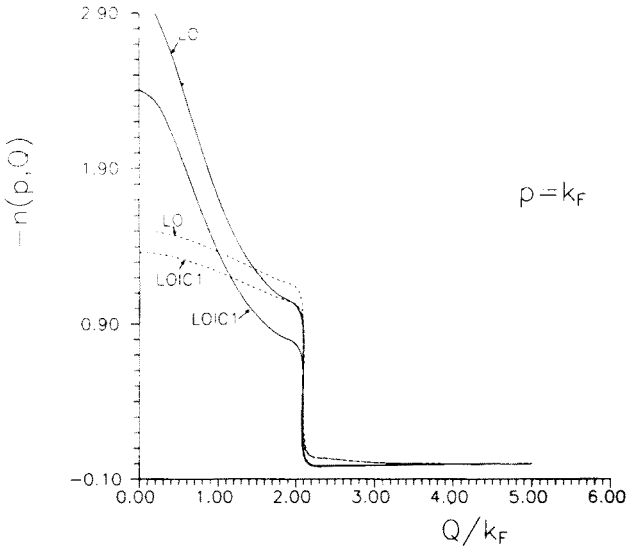


Fig. 12. Comparison of lowest-order (LO) and lowest-order irreducible-cluster (LOIC1) approximations to the generalized momentum distribution $n(\boldsymbol{p}, \boldsymbol{Q}\boldsymbol{p}/p)$, displayed as functions of $Q$ (with $Q > 0$ and $\boldsymbol{Q} \| \boldsymbol{p}$), at fixed $p = k_F$, for models MC (solid curves) and G2 (dashed curves). The corresponding result for the ideal Fermi gas is $-1$ for $Q/k_F \leq 2$ and zero otherwise.

some 17% to some 5% in the MC model and from about 7% to about 4% for G2, decreasing with increasing $Q$ in both models. The corresponding higher-order terms have a net positive effect.

We close this survey of numerical results with some data on the violations of the sequential relation by the LO and LOIC1 algorithms. To quantify these violations, we refer to the pertinent formulation (17) of the sequential condition and define a discrepancy measure $\Delta S$ in the LOIC1 case as the LOIC1 version of the left side of (17), minus the LOIC approximation to the right side, this difference being divided by $n_{\mathrm{LOIC}}(p)$ and given as a percentage; $\Delta S$ for the LO calculation is constructed in the same way in terms of LO quantities. At $p = k_F$, the results obtained for these measures are $\Delta S = -273\%$ (LO) and $= -192\%$ (LOIC1) when the MC model is employed and $\Delta S = -63\%$ (LO) and $= -47\%$ (LOIC1) in the G2 model. At $p = 2k_F$ the figures for the MC model are $\Delta S = +269\%$ (LO) and $-8\%$ (LOIC1). Judging from these examples, the higher-order terms contained in the LOIC1 treatment tend to decrease the violation of the sequential identity, but departures from this relation remain serious. It should of course be possible to devise a sequence of conserving approximations that meets the sequential condition in each order, by appropriate regroupings of individual Ursell–Mayer diagrams. However, it is to be expected that such

approximations will fail to satisfy some other identity or sum rule that is deemed important.

## 5. Conclusions and prospects

In this contribution we have presented and discussed a collection of results from an exploratory numerical study of the half-diagonal two-body density matrix $\rho_{2h}(\boldsymbol{r}_1, \boldsymbol{r}_2, \boldsymbol{r}_1')$ of symmetrical nuclear matter. These results have been expressed in terms of a Fourier transform $n(\boldsymbol{p}, \boldsymbol{Q})$ of $\rho_{2h}$, the generalized momentum distribution [29, 30] defined by Eq. (2). The calculations are based on a Jastrow–Slater ansatz for the ground-state wave function, and we have examined three versions of the state-independent Jastrow two-body correlation function $f(r)$, at densities near the empirical equilibrium density of the system. The results show interesting structural features arising from the statistical and geometrical correlations and their interplay. Significant deviations from the reference case of a noninteracting Fermi gas are observed in certain domains of the variables $\boldsymbol{p}$ and $\boldsymbol{Q}$, deviations which generally grow in importance with the size of the wound parameter $\kappa_{\mathrm{dir}} = \rho \int [f(r) - 1]^2 dr$.

It must be stressed that this work takes only the first steps toward a realistic calculation of $n(\boldsymbol{p}, \boldsymbol{Q})$ for infinite nuclear matter and accordingly will be subject to many refinements. For instance, there are indications that higher-order cluster corrections may have a stronger influence in $n(\boldsymbol{p}, \boldsymbol{Q})$ than was found to be the case for the analogous one-body quantity, the momentum distribution $n(p)$ [33]. In particular, we may point to the sensitive dependence of the deviations from the Fermi-gas result on $\kappa_{dir}$, as well as the violations of the sequential relation by the approximations employed, which can assume serious magnitude for realistic values of this parameter. It is naturally anticipated that convergence of the relevant cluster expansions will be worse, the larger the value of $\kappa_{\mathrm{dir}}$; however, in the present problem it would seem that the generally larger quantity $|\rho \int \zeta(r) dr| = |\rho \int [f(r) - 1] dr|$ may serve as a more appropriate "smallness parameter" for measuring the rapidity of cluster convergence. On the other hand, it is reassuring that the LOIC1 results for $n(\boldsymbol{p}, \boldsymbol{Q})$ at nonzero $Q$, which incorporate some higher-order cluster contributions relative to the LO treatment, show generally sensible agreement with the corresponding LO results. Even so, a quantitative comparison of LOIC1 and LO results points up the desirability or necessity of a more precise evaluation, through implementation of the available Fermi hypernetted-chain techniques [30] for resummation of the irreducible-diagram cluster series entering the Ristig–Clark structural formula (16) for the generalized momentum distribution. We are proceeding to carry through this program at the FHNC/0 level, to obtain a firmer basis for judging the efficacy of the more naive approximations.

Although FHNC — or alternatively stochastic computation — is the "algorithm of choice" from the standpoint of accurate determination of the generalized momentum distribution $n(\boldsymbol{p}, \boldsymbol{Q})$ for a Jastrow-Slater wave function, the formulation and testing of simple analytic or semi-analytic approximations remains an important goal, since it may be possible to adapt them more easily to the presence of state-dependent correlations and to phenomenological analyses of final-state interactions in finite nuclei. A similar strategy has proven successful in the case of the ordinary momentum distribution [42].

Further work along the lines we have identified should produce a quantitatively reliable description of the generalized momentum distribution, insofar as state-independent, central, two-body correlations play the dominant role. However, it is doubtless the case that a truly realistic description of $n(\boldsymbol{p}, \boldsymbol{Q})$ and the density matrix $\rho_{2h}(\boldsymbol{r}_1, \boldsymbol{r}_2, \boldsymbol{r}_1')$ over the full ranges of the momentum and spatial variables will require the introduction of state-dependent (spin-, isospin- and angle-dependent) correlations into the trial ground-state wave function of nuclear matter [48, 49]. As a significant step in this direction, the formalism developed by Ristig and Clark [29, 30] should be extended to a correlation operator appropriate to a nucleon-nucleon interaction of $v_6$ type [31, 49].

This paper is dedicated, with congratulations and best wishes, to our esteemed colleague and friend Janusz Dąbrowski on the occasion of his 65th Birthday. JWC would like to express his deep appreciation to Janusz for nearly thirty years of stimulating intellectual exchange on the nuclear-matter problem and countless other matters, and for valuable instances of congenial and constructive criticism. So many of us have been the beneficiaries of his wisdom, his warm fellowship, and his thoughtfulness.

The research reported herein has been supported in part by the Physics Division and the Division of Materials Research of the U. S. National Science Foundation under Grant No. PHY/DMR-9002863. EM thanks the University of Athens for partial financial support for a recent visit to Washington University, where she enjoyed the hospitality of the Department of Physics and the McDonnell Center for the Space Sciences. She is also grateful to W. H. Dickhoff, V. R. Pandharipande and R. Seki for very helpful discussions. We thank M. F. Flynn for providing FHNC data for $n(p)$ and $S(Q)$.

## REFERENCES


[1] J. Dąbrowski, *Proc. Phys. Soc.* **71**, 658 (1958).

[2] J. Dąbrowski, *Proc. Phys. Soc.* **72**, 499 (1958).

[3] B.D. Day, *Rev. Mod. Phys.* **39**, 719 (1967); H.A. Bethe, *Ann. Rev. Nucl. Sci.* **21**, 93 (1971); C. Mahaux, in *The Many-Body Problem: Jastrow Correlations versus Brueckner Theory*, Eds R. Guardiola, J. Ros, Springer-Verlag, Berlin 1981, p. 50.

[4] W.H. Dickhoff, H. Müther, *Rep. Prog. Phys.* **55**, 1947 (1992).

[5] R.F. Bishop, *Theor. Chim. Acta* **80**, 95 (1991).

[6] M.H. Kalos, P.A. Whitlock, *Monte Carlo Methods*, Vol. I, John Wiley & Sons, New York, 1986; *Monte Carlo Methods in Theoretical Physics*, Eds. S. Caracciolo, A. Fabrocini, ETS Editrice, Pisa, 1991.

[7] E. Feenberg, *Theory of Quantum Fluids*, Academic Press, New York, 1969.

[8] J.W. Clark, in *Progress in Particle and Nuclear Physics*, ed. D. H. Wilkinson, Pergamon Press, Oxford, 1979, Vol. 2, p. 89.

[9] J.W. Clark, E. Krotscheck, in *Recent Progress in Many-Body Theories*, ed. H. Kümmel, M. L. Ristig, Springer–Verlag, Berlin, 1984, p. 127.

[10] S. Fantoni, V.R. Pandharipande, *Phys. Rev.* **C37**, 1697 (1988).

[11] A. Ramos, A. Polls, W.H. Dickhoff, *Nucl. Phys.* **A503**, 1 (1989); B.E. Vonderfecht, W.H. Dickhoff, A. Polls, A. Ramos, *Phys. Rev.* **C44**, R1265 (1991); B.E. Vonderfecht, W.H. Dickhoff, A. Polls, A. Ramos, *Nucl. Phys.*, in press.

[12] O. Benhar, A. Fabrocini, S. Fantoni, *Nucl. Phys.* **A505**, 267 (1989); *Phys. Rev.* **C41**, R24 (1990); and *Nucl. Phys.* **A**, in press.

[13] H.S. Köhler, *Nucl. Phys.* **A537**, 64 (1992); *Phys. Rev.* **C46**, 1687 (1992).

[14] M. Baldo, I. Bombaci, G. Giansiracusa, U. Lombardo, C. Mahaux, R. Sartor, *Nucl. Phys.* **A545**, 741 (1992).

[15] S.C. Pieper, R.B. Wiringa, V.R. Pandharipande, *Phys. Rev. Lett.* **64**, 364 (1990).

[16] S. Stringari, *Phys. Rev.* **B46**, 2974 (1992); and references therein.

[17] F. Dalfovo, S. Stringari, *Phys. Rev. Lett.* **63**, 532 (1989).

[18] *Momentum Distributions*, Eds R.N. Silver, P.E. Sokol, Plenum Press, New York, 1989.

[19] M.L. Ristig, J.W. Clark, in *Recent Progress in Many-Body Theories*, Ed. Y. Avishai, Plenum Press, New York, 1990, Vol. 2, p. 323.

[20] B. Frois, C. Papanicolas, *Ann. Rev. Nucl. Part. Sci.* **37**, 133 (1987); D.B. Day, J.S. McCarthy, T.W. Donnelly, I. Sick, *Ann. Rev. Nucl. Part. Sci.* **40**, 357 (1990).

[21] D.K.A. de Witt Huberts, *J. Phys. G* **16**, 507 (1990); D.F. Geesaman *et al.*, *Phys. Rev. Lett.* **63**, 734 (1989); G. Garino *et al.*, *Phys. Rev.* **C45**, 780 (1991); NE.18 experiment, SLAC, under analysis; Letter of Intent, SLAC End Station A, Nov. 1991.

[22] A.S. Carroll *et al.*, *Phys. Rev. Lett.* **61**, 1698 (1988); Brookhaven AGS proposal E850, A.S.Carroll, S. Heppelmann, spokespersons.

[23] D. Ashery, J. Schiffer, *Ann. Rev. Nucl. Part. Sci.* **36**, 207 (1986).

[24] O. Benhar, A. Fabrocini, S. Fantoni, G.A. Miller, V.R. Pandharipande, I. Sick, *Phys. Rev.* **C44**, 2328 (1991).
[25] A. Kohama, K. Yazaki, R. Seki, to appear in *Nucl. Phys.* **A**.
[26] J.W. Clark, R.N. Silver, in *Proceedings of the Third International Conference on Nuclear Reaction Mechanisms*, ed. E. Gadioli, Universitá degli Studi di Milano 1988, p. 531; and references therein.
[27] C. Ciofi degli Atti, E. Pace, G. Salme, *Phys. Rev.* **C43**, 1155 (1991).
[28] A.S. Rinat, W.H. Dickhoff, *Phys. Rev.* **B42**, 10004 (1990).
[29] M.L. Ristig, J.W. Clark, *Phys. Rev.* **B40**, 4355 (1989).
[30] M.L. Ristig, J.W. Clark, *Phys. Rev.* **B41**, 8811 (1990).
[31] J.W. Clark, in *The Many-Body Problem: Jastrow Correlations versus Brueckner Theory*, Eds R. Guardiola, J. Ros, Springer-Verlag, Berlin, 1981, p. 184.
[32] P.M. Lam, J.W. Clark, M.L. Ristig, *Phys. Rev.* **B16**, 222 (1977).
[33] M.F. Flynn, J.W. Clark, R.M. Panoff, O. Bohigas, S. Stringari, *Nucl. Phys.* **A427**, 253 (1984).
[34] S. Fantoni, V.R. Pandharipande, *Nucl. Phys.* **A427**, 473 (1984).
[35] A. Ramos, W.H. Dickhoff, A. Polls, *Phys. Rev.* **C43**, 2239 (1991).
[36] C. Mahaux, R. Sartor, *Phys. Rep.* **211**, 53 (1992).
[37] R. Schiavilla, V.R. Pandharipande, R.B. Wiringa, *Nucl. Phys.* **A449**, 219 (1986).
[38] A.N. Antonov, P.E. Hodgson, J.Zh. Petkov, in *Nucleon Momentum and Density Distributions in Nuclei*, Clarendon Press, Oxford, 1988.
[39] H.A. Gersch, L.J. Rodriguez, P.N. Smith, *Phys. Rev.* **A5**, 1547 (1972); R.N. Silver, *Phys. Rev.* **B38**, 2283 (1988); A.S. Rinat, *Phys. Rev.* **B40**, 6625 (1989).
[40] D.M. Ceperley, in *Momentum Distributions*, Ed. R.N. Silver, P.E. Sokol, Plenum Press, New York, 1989, p. 71.
[41] C. Carraro, S.E. Koonin, *Nucl. Phys.* **A524**, 201 (1991); C. Carraro, R. Seki, T. Shoppa, unpublished.
[42] S. Stringari, M. Traini, O. Bohigas, *Nucl. Phys.* **A516**, 33 (1990).
[43] M.L. Ristig, J.W. Clark, *Phys. Rev.* **B14**, 2875 (1976).
[44] D. Ceperley, G.V. Chester, M.H. Kalos, *Phys. Rev.* **B16**, 3081 (1977).
[45] V.R. Pandharipande, R.B. Wiringa, B.D. Day, *Phys. Lett.* **B57**, 205 (1975).
[46] A. Ramos, W.H. Dickhoff, A. Polls, *Phys. Lett.* **B219**, 15 (1989).
[47] E. Mavrommatis, J.W. Clark, in *Condensed Matter Theories*, Ed. V.C. Aguilera-Navarro, Plenum Press, New York, 1990, Vol. 5, p. 97.
[48] M.L. Ristig, W.J. Ter Louw, J.W. Clark, *Phys. Rev.* **C3**, 1501 (1971); *Phys. Rev.* **C5**, 695 (1972).
[49] V.R. Pandharipande, R.B. Wiringa, *Rev. Mod. Phys.* **51**, 821 (1979).